Strong-motion characteristics in Sendai city during the 2011 Tohoku earthquakes, Japan

S. Ohno, M. Motosaka & A. Shibayama
Tohoku University, Sendai, Japan

K. Mitsuji
Yamagata University, Yamagata, Japan

SUMMARY
We investigate the strong-motion characteristics in Sendai, the largest city in the damaged area during the 2011 M9.0 Tohoku earthquake, Japan, using the DCRC strong-motion network records. Strong-motion duration of the 2011 Tohoku earthquake is significantly longer than that of the M7.4 1978 Miyagi-oki earthquake, but the spectral amplitudes of the 2011 earthquake in the range of 0.02-10 seconds were about 1.3 times as large as those of the 1978 earthquake at most. Distributions of strong-motion spectra are estimated for the 2011 Tohoku earthquake sequences by using all currently available strong-motion records including the DCRC records and a subsurface structure model in Sendai. Short-period (less than 1s) amplitudes are predominant at northwest area, while not only short but also long-period (around 3s) amplitudes are predominant at southern area of Sendai. Period-dependent predominant directions are also investigated.

Keywords: The 2011 Tohoku earthquake, Sendai, Strong-Motion, Soil Amplification, Predominant Direction

1. INTRODUCTION

During the 3/11/2011 Tohoku earthquake (M9.0), large accelerations were observed over the wide area along Pacific coast of Tohoku district, Japan. In the damaged area, Sendai is the largest city and had experienced the 1978 Miyagi-oki earthquake (M7.4). We have been conducting strong-motion observation in Sendai since 2004, and we obtained earthquake records during the fore, main and aftershocks of the 2011 Tohoku earthquake sequences. In this paper, we investigate the strong-motion characteristics in Sendai concerning spatial spectral distributions and predominant directions mainly based on our strong-motion network records.

2. STRONG-MOTION NETWORKS AND UNDERGROUND STRUCTURE IN SENDAI

Fig.1 shows the location of observation stations in Sendai. There are two major strong ground motion networks in Sendai: Small Titan by Tohoku Institute of Technology (Shoji and Kamiyama, 2000; Kamiyama *et al.*, 2011) and DCRC network by Disaster Control Research Center of Tohoku University (Ohno *et al.*, 2004). Almost all DCRC stations are located on the 1st floor of low-rise buildings (simultaneous observation with top floor at some places).

Sendai has a complicated subsurface structure. Fig. 2 shows the depth distributions of engineering bedrock (S-wave velocity of 0.7km/s) and seismic bedrock (S-wave velocity of 3.0km/s) of subsurface structure model used for earthquake damage estimation in Sendai (Sendai City, 2002).

Nagamachi-Rifu fault, a reverse-type active fault dipping to NW direction, crosses the central part of city area in NE-SW direction. The west side of the fault is terrace and the east side is lowland (alluvial deposits). Thickness of surface soil shallower than engineering bedrock at the ease side of the fault is up to 80m and deeper than that at the west side. On the other hand, thickness of the deep part of subsurface structure (from ground surface to seismic bedrock) becomes deeper from east to west (Watanabe and Motosaka, 2002).

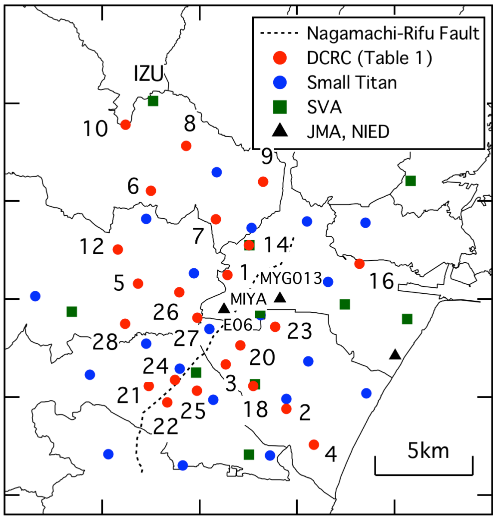

Figure 1. Location of DCRC strong-motion stations in Sendai

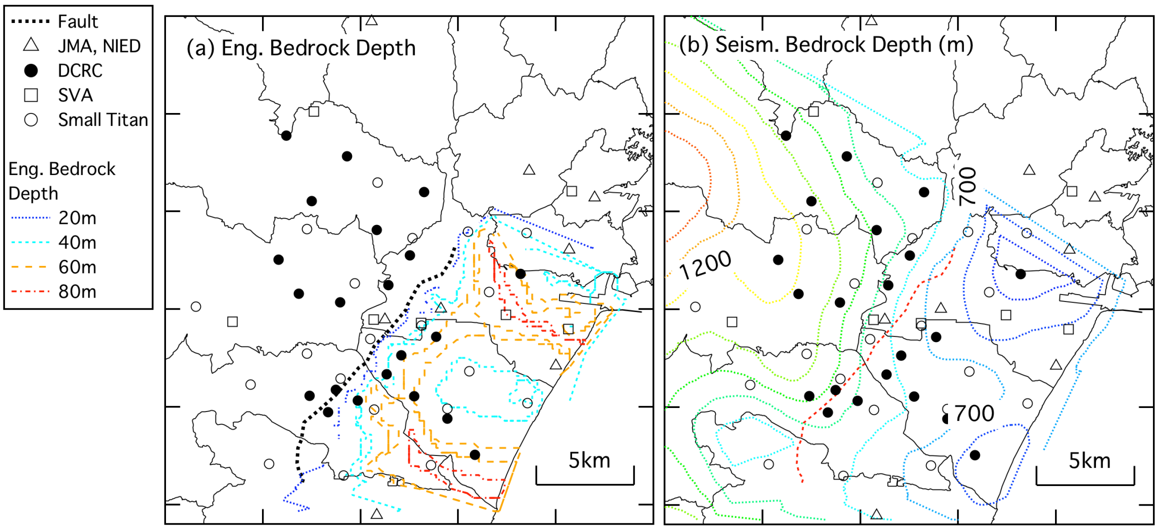

Figure 2. Depths of engineering bedrock and seismic bedrock in Sendai (Sendai City, 2002)

3. STRONG-MOTION RECORDS DURING THE 2011 TOHOKU EARTHQUAKE

Table 1 shows a list of observation records by the DCRC network for the 3/9 foreshock, 3/11 mainshock, 4/7 and 4/11 aftershocks. During the 3/11 mainshock, records at 14 of 21 stations were obtained. PGA and PGV range 318-840 Gal and 30-88 cm/s, respectively. The largest acceleration (822Gal) and seismic intensity (6.2) in the DCRC network was observed at No.9. At the other organizations, 1517 Gal was observed at K-NET MYG013, where boil sand and acceleration spikes probably due to soil liquefaction were observed. Also, the largest acceleration observed in the Small Titan network was 1853 Gal at Nanakita junior high school (NAKI), and the largest seismic intensity was 6.5 at Shichigo junior high school (CCHG) (Kamiyama *et al.*, 2011). In Sendai, the 4/7 aftershock also caused severe damage, as did the mainshock. PGA and PGV of this aftershock range 167-767 Gal and 14-76 cm/s, respectively.

Table 1. List of earthquake records by the DCRC strong-motion network, Tohoku University

		Origin Time (JST)	2011/4/11			2011/4/7			2011/3/11			2011/3/9		
		Area	Eastern Fukushima Pref.			Off Miyagi Pref.			2011 Tohoku Eq.			Far E Off Miyagi Pref.		
		Mw, Depth	Mw 6.6, Depth 6km			Mw 7.1, Depth 66km			Mw 9.0, Depth 24km			Mw7.2, Depth 8km		
		Type	Shallow Inland			IntraSlab			Subduction			Subduction		
No	Sensor	Station	PGA (cm/s^2)	PGV* (cm/s)	JMA Int.	PGA (cm/s^2)	PGV* (cm/s)	JMA Int.	PGA (cm/s^2)	PGV** (cm/s)	JMA Int.	PGA (cm/s^2)	PGV* (cm/s)	JMA Int.
2	ETNA	Rokugo Elementary School	54	5.5	3.9	311	42.1	5.7	No Record			No Record		
3	ETNA	Furujiro Elementary School	48	7.3	3.7	251	22.4	5.1	320	59.5	5.7	24	3.1	3.3
4	ETNA	Higashi Rokugo Elementary School	Removed			Removed			613	74.2	6.0	29	3.4	3.4
5	QDR	Daiichi Jr. High School	47	6.3	3.8	230	19.3	5.1	383	39.4	5.6	28	2.9	3.5
8	QDR	Shogen-Chuoh Elementary School	76	5.3	3.9	534	25.3	5.5	840	60.4	6.0	30	2.2	3.2
9	QDR	Matsumori Elementary School	No Record			767	75.5	6.2	822	85.7	6.4	46	4.2	3.7
10	QDR	Miyagi Prefecture Library 1F	No Record			279	18.0	5.0	407	62.7	5.6	20	2.4	3.2
12	QDR	Seiryo SecondarySchool 1F	30	5.4	3.7	No Record			No Record			19	3.5	3.3
14	QDR	Tsurugaya Elementary School 1F	48	4.3	3.5	432	30.6	5.7	No Record			20	1.9	3.1
16	QDR	Nakano Jr. High School 1F	81	7.8	4.3	No Record			No Record			40	3.2	3.6
18	QDR	Okino Elementary School 1F	71	6.9	4.1	360	31.8	5.6	512	77.6	6.2	37	3.5	3.5
20	QDR	Minami Koizumi Elementary School	34	6.6	3.6	220	25.7	5.3	381	63.0	5.6	19	2.4	3.1
21	QDR	Nishitaga Jr. High School	54	6.4	3.9	186	16.4	5.0	400	45.1	5.5	23	3.0	3.4
22	QDR	Tomizawa Jr. High School	53	8.8	3.9	232	21.1	5.2	416	54.6	5.7	29	3.2	3.4
23	QDR	East Water Supply Center	95	6.0	4.1	472	37.3	5.8	613	75.4	6.1	30	2.6	3.3
24	QDR	Ryutaku-Ji	Removed			Removed			No Record			No Record		
25	QDR	Nagamachi Minami Community Center	No Record			264	29.5	5.5	494	69.3	6.0	59	6.0	4.0
26	QDR	Aoba Ward Office	43	6.0	3.7	318	21.9	5.2	No Record			24	3.2	3.3
27	SSA-1	Sumitomo Seimei Bldg.	31	3.9	3.5	167	14.0	4.9	318	29.2	5.3	15	2.2	3.1

* cut-off period of 10s, ** cut-off period of 10s, ** 50s

Fig. 3 shows the mainshock velocity waveforms in observation components near NS direction at all DCRC stations, with JMA E06, K-NET MYG013, and ground station of Izumi electric power building (IZU), Tohoku Electric Power Co. Velocity waveforms in Fig. 3 are calculated from acceleration records with low-cut frequency of 0.02Hz. Two major wave groups (hereafter Part A and Part B of the mainshock) can be commonly identified. There are gaps in waveforms at some QDR stations. This gap is due to the limitation of QDR that the record length of one file is up to 100s.

Fig. 4 compares pseudo velocity response spectra (5% damping) at stations locating east and west sides of Nagamachi-Rifu fault. The spectrum at No.27, locating near Sendai railway station, is commonly plotted in each side as a reference, because this station locates on the engineering bedrock (Ohno *et al.*, 2012a). Spectra at west sides are equal to or relatively larger at short period (less than 1 second) than the No.27 spectrum, while the spectra at east sides are significantly larger than the No.27 spectrum, especially at around 1 and 3 seconds. Such difference can be generally explained by the differences of site amplifications due to subsurface structure (Ohno *et al.*, 2012b).

Fig. 5 and fig. 6(a) compare acceleration waveforms and pseudo velocity response spectra at No.27 for the 2011 Tohoku earthquake (M9.0) with the 1978 Miyagi-oki earthquake (M7.4). Strong-motion duration of the 2011 mainshock is about 3 minutes, which is significantly longer than that of the 1978 earthquake. On the other hand, the spectral amplitudes of the 2011 mainshock in the range of 0.02-10 seconds were about 1.3 times as large as those of the 1978 earthquake at most. Fig. 6(a) also indicates that the 4/7 aftershock amplitude at around 1-2s is almost the same as that of the mainshock.

Fig. 6(b) compares pseudo velocity response spectra in NS component for 5 major earthquakes from the 8/16/2005 Miyagi-oki (M7.2) to the 4/11/2011 aftershock at No.25. Two predominant periods (around 3s and less than 1s) can be identified and the shorter predominant period clearly shows dependency on the amplitude level. This site is located on alluvial deposits, and such amplitude-dependent period change can be explained due to the nonlinearity of the surface soil (Ohno *et al.*, 2012a). Also, the 3-sec peak is affected by surface waves due to deep irregular underground structure (Ohno *et al.*, 2012b), as clearly shown in the later phase at No.25 in Fig. 3.

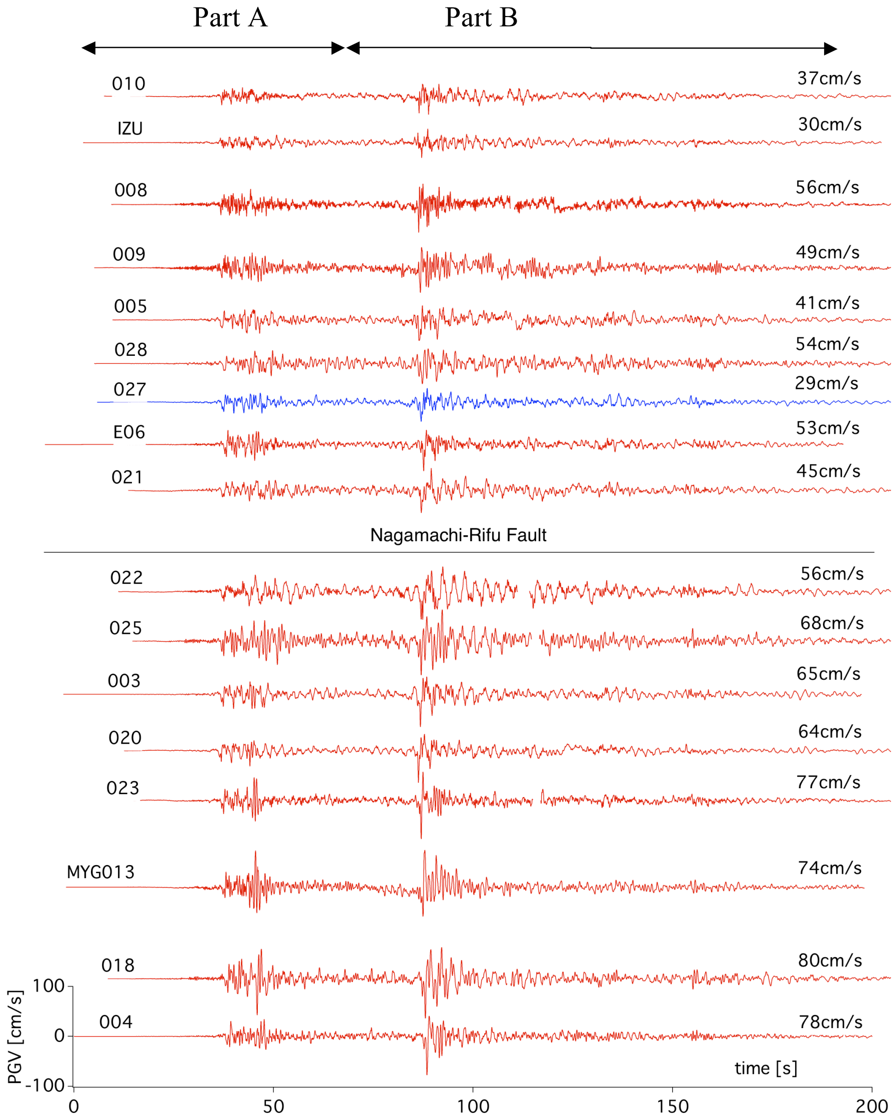

Figure 3. Velocity waveforms of the DCRC records for the 2011 Tohoku earthquake

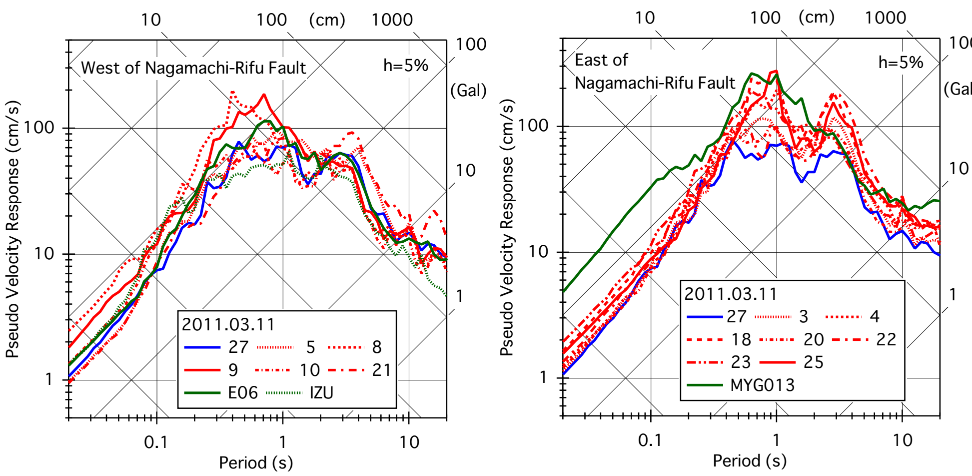

Figure 4. Pseudo velocity response spectra of the DCRC records for the 2011 Tohoku earthquake

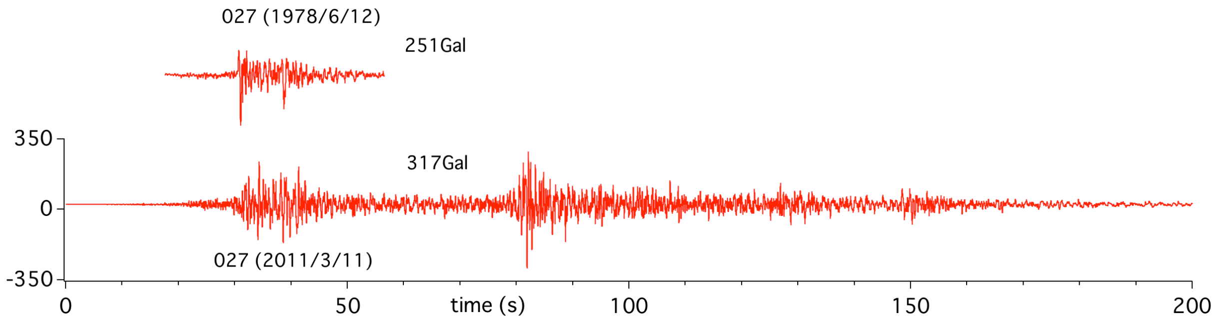

Figure 5. Acceleration waveforms at No.27 station for the 1978 Miyagi-oki and 2011 Tohoku earthquakes

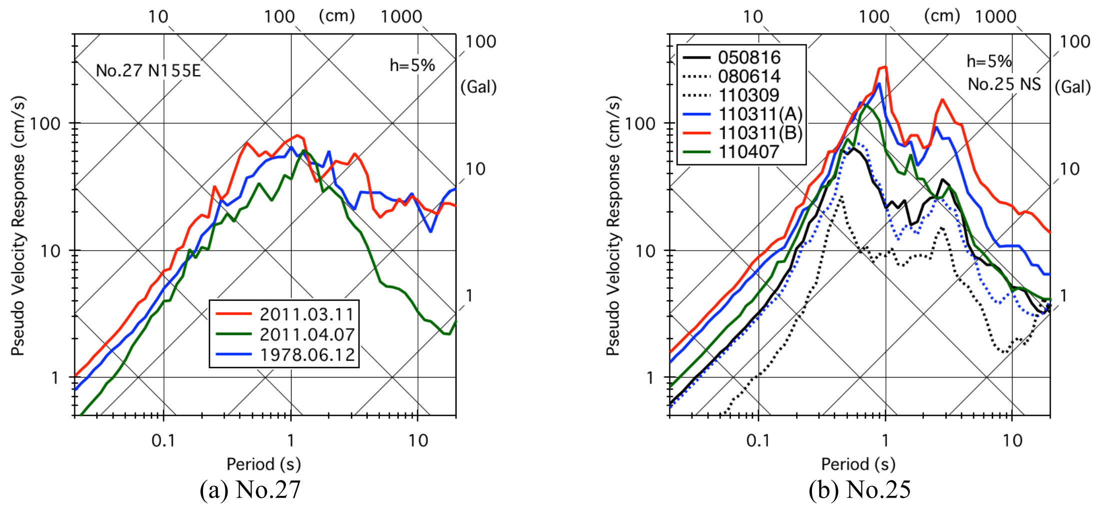

Figure 6. Pseudo velocity response spectra at No.27 and No.25 stations

4. STRONG-MOTION CHARACTERISTICS IN SENDAI

Spatial characteristics of spectral amplitudes as well as directions of strong-motions are important to investigate structural damages. We estimate the distributions of pseudo velocity response spectra and predominant directions in Sendai, using the records of not only DCRC, but also TOHTECH, NIED, NILIM, PARI, JMA, BRI, Sendai City, Miyagi Pref., and Tohoku Electric Power Company.

4.1 Spectral Distributions

Using the method of Ohno and Shibayama (2010), we estimate distribution of response spectra at ground surface in 250m-mesh over the city area of Sendai. Fig. 7 shows a flowchart of the method, which takes into account the effects of subsurface structure including nonlinear amplification of surface soil and spatial correlation of the spectra. The procedure is composed of 3 steps: 1) estimate response spectra at outcropped seismic bedrock at observation station location, by recursively applying equivalent linear spectral modal analysis of 1-D subsurface structure (linear analysis for the part deeper than engineering bedrock), 2) estimate spatial correlation of outcropped spectra and interpolate in 250m-mesh by ordinary kriging method, 3) estimate ground surface spectrum in each mesh by equivalent linear spectral modal analysis.

We used the subsurface structure model (including nonlinear soil properties of soil) in Sendai City (2002). Fig. 8 and Fig. 9 show the estimation results at periods of 0.2, 1, and 3.2s for parts A and B of the mainshock, and for the 4/7 and 4/11 aftershocks. These periods are selected as representatives of important periods to nonstructural damage, low-rise building, and middle-height and base-isolated buildings, respectively. Black dots indicate the stations. The following tendencies are found:

1) Strong-shaking areas are different by period: (a) At 0.2s, amplitude at the northwestern area is larger than the other area. This is due to the shallow soil over engineering bedrock. An exception is the 4/11 shallow inland aftershock, probably due to the lack of short-period incident waves by strong attenuation in propagating the shallow crust. (b) At 1.0s, amplitudes at the eastern side of Nagamachi-Rifu fault are larger, due to the surface soil amplification. (c) At 3.2s, amplitudes at the southern area are larger, due to the deep underground structure including existence of surface waves as discussed before. The 4/11 aftershock again shows a different distribution. In this earthquake, large amplitude area expands from southern side to northwestern side. Similar distribution was found for the 6/14/2008 Iwate-Miyagi-Nairiku shallow inland earthquake (Ohno and Shibayama, 2010).

2) The amplitudes of Part B are generally larger than those of Part A during the mainshock.

3) Amplitudes at NS direction are larger than those at EW direction during the mainshock (both parts A and B), while EW direction is predominant at the 4/7 aftershock. At the 4/11 aftershock, NS direction is significantly predominant at long periods.

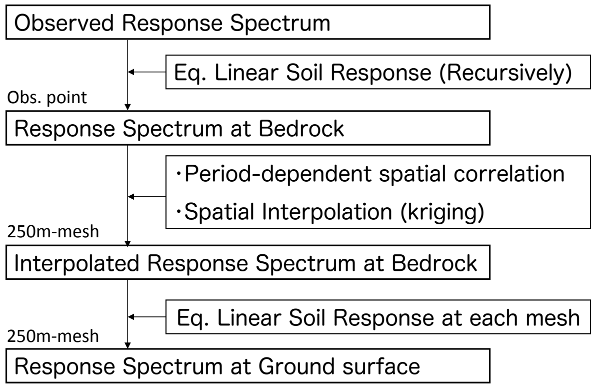

Figure 7. Flowchart of estimating distribution of response spectra in Sendai (Ohno and Shibayama, 2010)

4.2 Predominant Directions

Fig. 10 shows predominant directions of horizontal motion of bandpass filtered waves at three period ranges. The center periods of the filter are the same as the periods in Figs. 8 and 9, and their short and long cut-off periods are $1/\sqrt{2}$ and $\sqrt{2}$ times as the center period, respectively. The predominant direction is estimated by the polarization analysis of particle motion (Vidale, 1986). The direction of principal axis at the time of maximum eigenvalue is plotted in each figure. The line length is the same at each station (only its direction is shown). From this figure, the following tendencies are found:

1) At 0.2s, the predominant directions are scattered for all earthquakes.

2) At 1.0s, N-S and SE-NW directions are commonly predominant in the central and south area of Sendai during the mainshock (both parts A and B), while E-W direction is predominant in the central area at the 4/7 aftershock.

3) At 3.2s, E-W direction is predominant in the north and west area, while NS to NW-SE directions are predominant in the south and southeast area for parts A and B of the mainshock. EW-direction is predominant for the 4/7 earthquake, while NS-direction is predominant for the 4/11 earthquake.

These tendencies need to be numerically investigated in relation to irregular subsurface structure and source location.

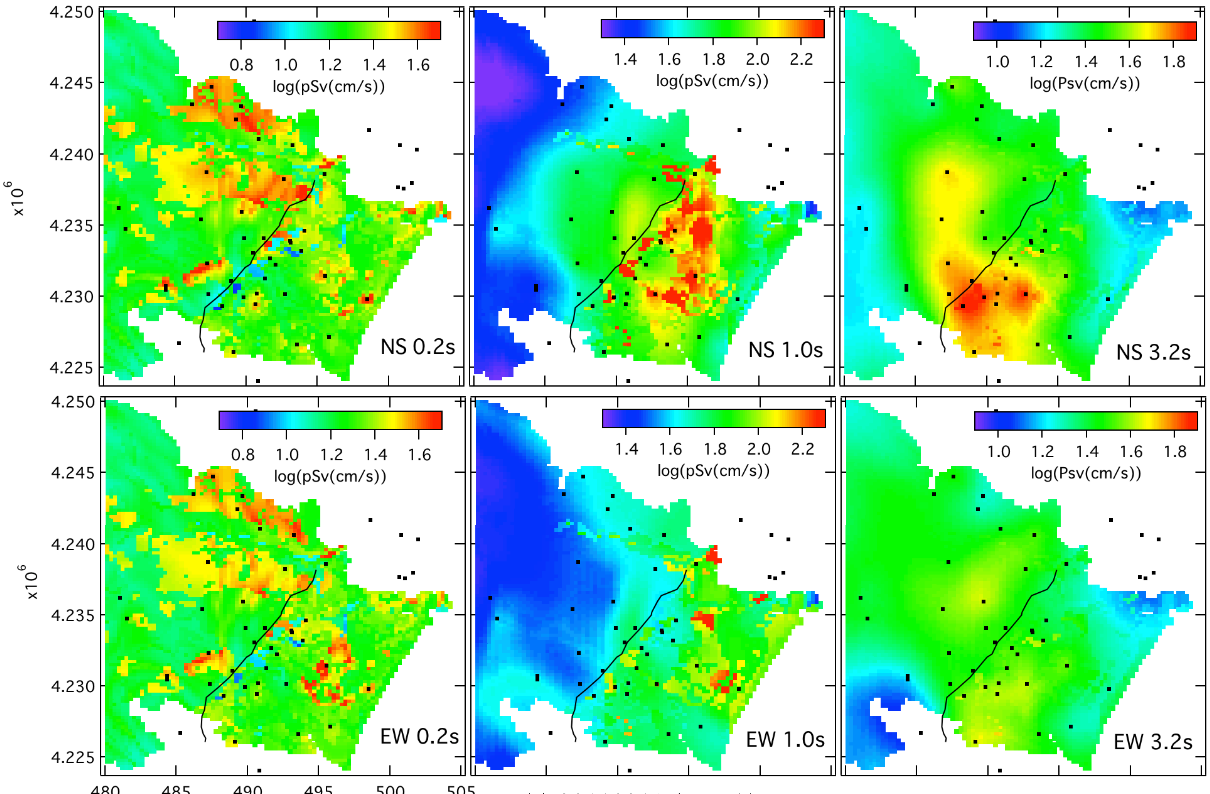

(a) 20110311 (Part A)

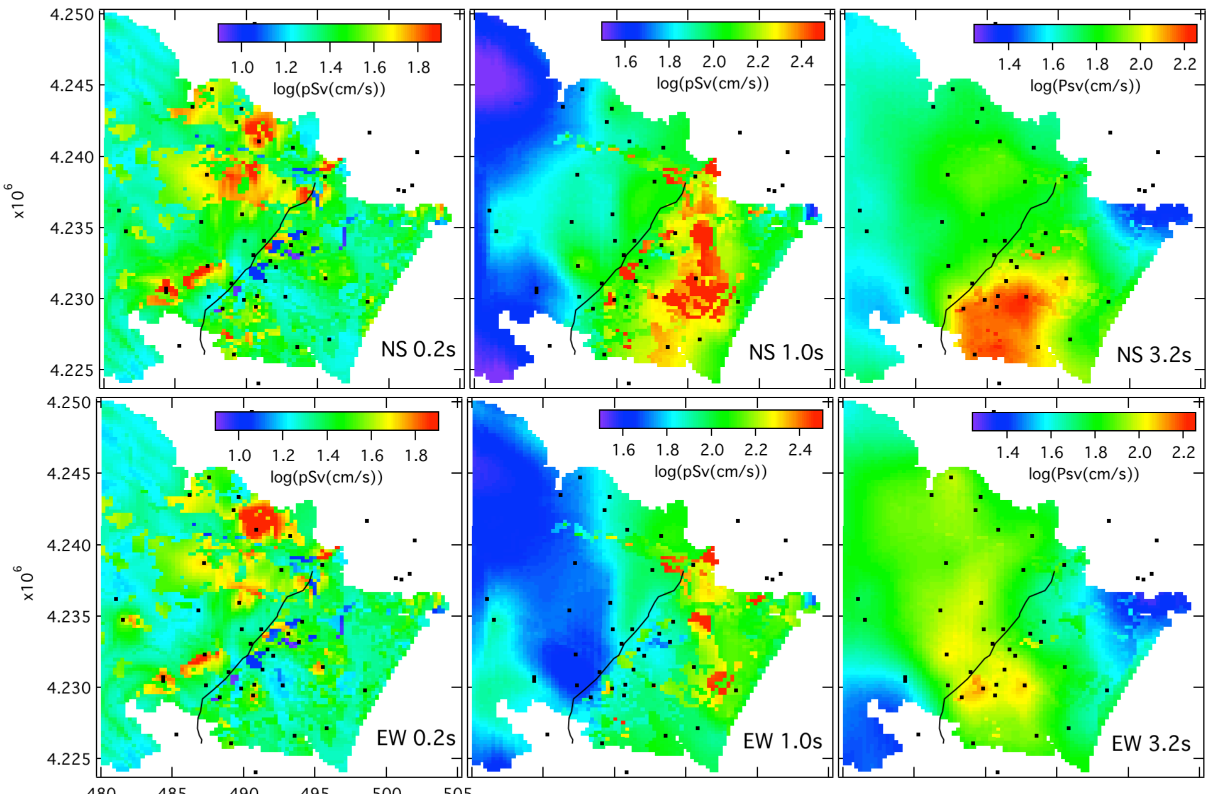

(b) 20110311 (Part B)

Figure 8. Estimated distribution of response spectra at ground surface for the 2011 Tohoku earthquake

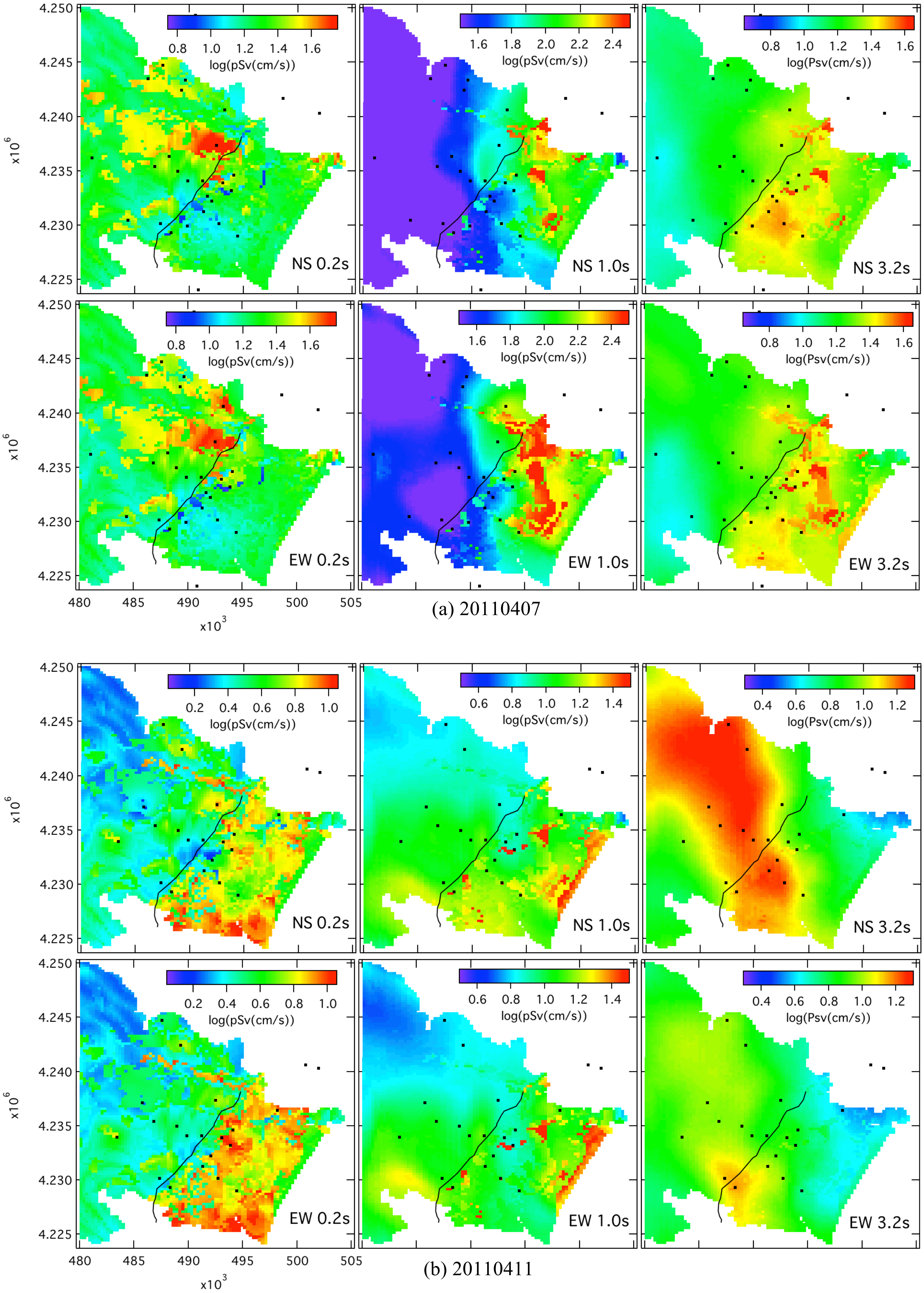

Figure 9. Estimated distribution of response spectra for the aftershocks of the 2011 Tohoku earthquake

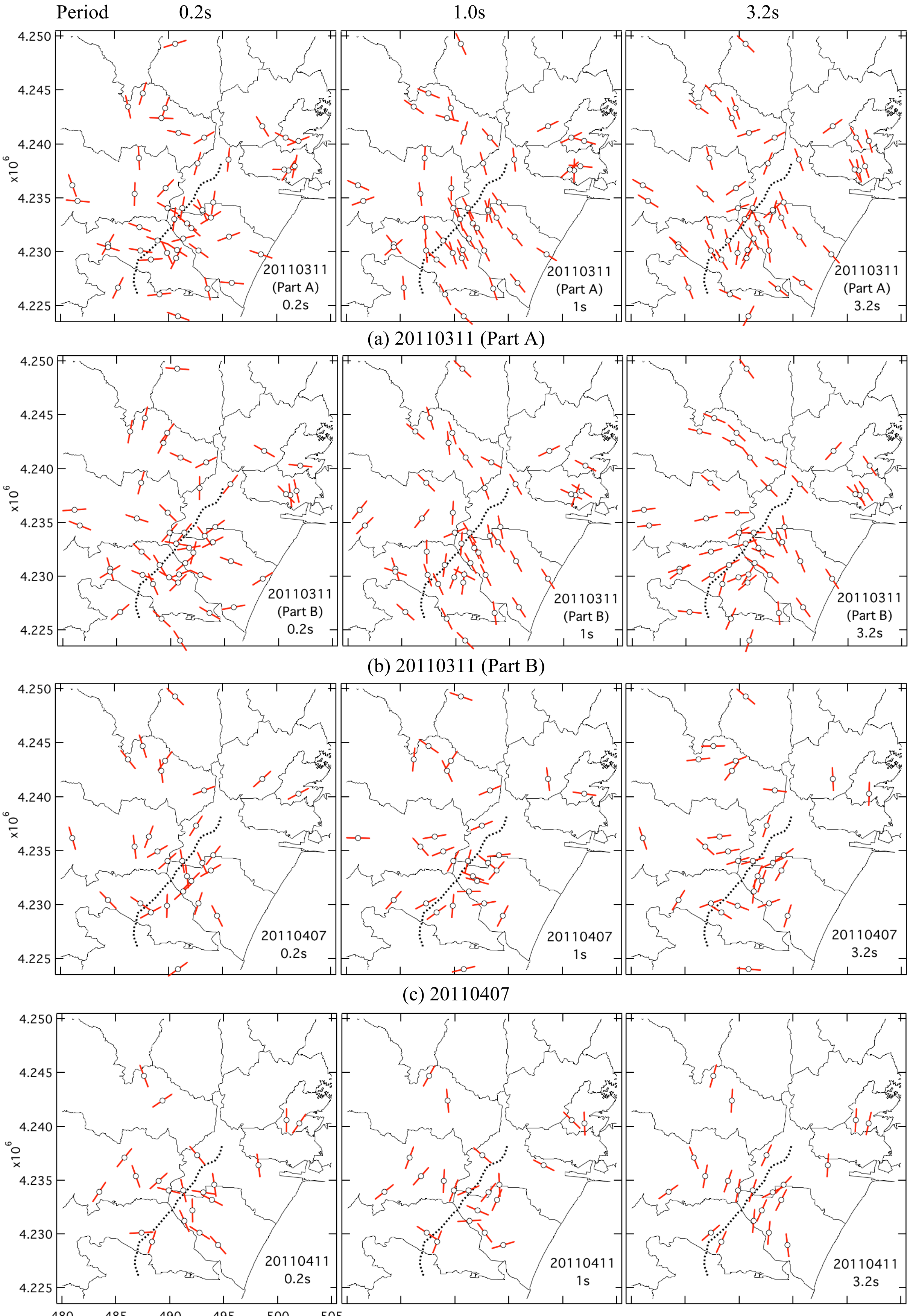

Figure 10. Period-dependent predominant directions for the 2011 Tohoku earthquake and its aftershocks

5. CONCLUSIONS

We investigate the strong-motion characteristics in Sendai, Japan, for the 2011 Tohoku earthquake sequences. The following conclusions are obtained:

1) Strong-motion duration of the 2011 Tohoku earthquake is significantly longer than that of the M7.4 1978 Miyagi-oki earthquake, but the spectral amplitudes of the 2011 earthquake in the range of 0.02-10 seconds were about 1.3 times as large as those of the 1978 earthquake at most.

2) Distributions of strong-motion spectra are estimated for the 2011 Tohoku earthquake sequences by using all currently available strong-motion records including the DCRC network records and a subsurface structure model in Sendai. Short-period (less than 1s) amplitudes are predominant at northwestern area, while not only short but also long-period (around 3s) amplitudes are predominant at southern area of Sendai.

3) At period of around 1s, which is important to structural damage for low-rise buildings, NS direction is predominant during the mainshock, but EW direction is predominant at the 4/7 aftershock.

ACKNOWLEDGMENTS

Strong motion records from Tohoku Institute of Technology (TOHTECH), National Research Institute for Earth Science and Disaster Prevention (NIED), National Institute for Land and Infrastructure Management (NILIM), Port and Airport Research Institute (PARI), Japan Meteorological Agency (JMA), Building Research Institute (BRI), Sendai City, Miyagi Pref., and Tohoku Electric Power Company are used for the estimation of spectral distribution and predominant direction.

REFERENCES

Building Research Institute and Japan Association for Building Research Promotion (1999). Sendai high-density strong-motion array comprehensive report. (in Japanese)

Shoji, Y. and Kamiyama, M. (2000). A High-Density Array Observation System Small-Titan: An Introduction and It's Strong-Motion Records, *Proc. 12WCEE*, 1-8.

Kamiyama, M., Matsuzawa, T. and M. Anazawa (2011). Strong-Motion Records Obtained by Small-Titan of Tohoku Institute of Technology During the 2011 Great East Japan Earthquake, *Quick Report Version 1 Issued for the Tohoku Branch of the Japanese Geotechnical Society*.

Ohno, S., Motosaka, M., Sato, T. and Yamamoto, Y. (2004). Strong-motion Observation Network for Seismic Capacity Evaluation of Buildings in Sendai, Japan, *Summaries of Technical Papers of Annual Meeting, Architectural Institute of Japan,* Structures, **Vol. II**, 1075-1076. (in Japanese)

Ohno, S. and Shibayama, A. (2010). Estimation of spatial distribution of response spectra considering soil amplification and spatial correlation of ground motions, *Proc. 13th Japan Earthquake Engineering Symposium*, GO1-Thu-PM-10. (in Japanese with English Abstract)

Ohno, S., Motosaka, M., Kazuya, M. and Shibayama, A. (2012a) Site Response Characteristics in Sendai City Estimated from Acceleration Records of the 2011 Tohoku Earthquake, Japan, *Proc. of the International Symposium on Engineering Lessons Learned from the 2011 Great East Japan Earthquake*, Paper No. 119.

Ohno, S., Mitsuya, E. and Motosaka, M. (2012b) Site Amplification Characteristics in Sendai City during the 2011 Tohoku Earthquake, Japan, *Journal of Japan Association for Earthquake Engineering* (in Japanese with English Abstract, submitted).

Sendai City (2002). Heisei 14 Fiscal Year Earthquake Damage Estimation Report. (in Japanese)

Vidale, J. E. (1986) Complex polarization analysis of particle motion, *Bull. Seism. Soc. Am.*, **76**, 1393-1405.

Watanabe, T. and Motosaka, M (2002). Estimation of Deep Underground Structure in Sendai Area based on Microtremor Observations and Strong-motion Prediction, *Proc. AIJ Tohoku Chapter Architectural Research Meeting*, **65**, 133-136. (in Japanese)